Food and Chemical Toxicology 132 (2019) 110655

Contents lists available at ScienceDirect

Food and Chemical Toxicology

journal homepage: www.elsevier.com/locate/foodchemtox

Methyl protodioscin from *Polygonatum sibiricum* inhibits cervical cancer through cell cycle arrest and apoptosis induction

Yi-Long Ma[a,1], Ying-Shuo Zhang[a,1], Fan Zhang[a], Yuan-Yuan Zhang[a], Kiran Thakur[a], Jian-Guo Zhang[a], Zhao-Jun Wei[a,b,*]

[a] School of Food Science and Biological Engineering, Hefei University of Technology, Hefei, 230009, People's Republic of China
[b] Anhui Province Key Laboratory of Functional Compound Seasoning, Anhui Qiangwang Seasoning Food Co., Ltd, Jieshou, 236500, People's Republic of China

ARTICLE INFO

Keywords:
Polygonatum sibiricum
Methyl protodioscin
Cell cycle
Apoptosis
Molecular mechanism

ABSTRACT

Methyl protodioscin (MPD) is a steroid saponin which has been well known for its pharmacological properties. Herein, we evaluated the anti-cancer activity of MPD for proliferation inhibition and apoptosis induction in Hela cells. MPD was purified from the rhizoma of *Polygonatum sibiricum* primarily and identified by HPLC, UPLC-TOF-MS/MS and NMR analysis, respectively. Results showed that MPD repressed cell proliferation at IC_{50} of 18.49 μM, altered cell morphology, arrested the cell cycle in G2/M phase, facilitated the generation of intracellular ROS and led to cell apoptosis in a concentration-dependent manner. Furthermore, MPD treatment promoted death receptor pathway and mitochondrial pathway efficiently. The inhibition of Caspase-8 and Caspase-9 proteins in these pathways abolished the apoptosis significantly, further demonstrated the mechanism of MPD-induced apoptosis. These findings offer novel information that MPD may be considered as a possible natural anti-cancerous agent in the form of functional foods or medicinal products.

1. Introduction

Cervical cancer occurs as third highest incidence in a global context and is considered as the most common gynecological cancer in developing countries (Tsikouras et al., 2016). Single or combined surgery, chemotherapy, and radiation are commonly used for the treatments of the disease. However, a high percentage of cancer patients are still challenged with relapse after treatment and may be accompanied by a sequence of serious side effects (Daniyal et al., 2015). Therefore, it is urgent to find natural anti-cervical cancer component with obvious anti-cancer effect and hypotoxicity.

Apoptosis plays a crucial role in the evolution of organisms, the maintenance of homeostasis, and the development of multiple systems (Kiraz et al., 2016). It involves the activation, expression, and regulation of a variety of genes. A large number of literatures have confirmed the regulatory mechanism of various factors, such as B-cell lymphoma-2 (Bcl-2) family and caspase family in cell apoptosis (Lin et al., 2012). Consequently, the exploration of apoptosis-inducing compounds and the investigation of their molecular mechanisms are the key points in developing anticancer drugs.

Polygonatum sibiricum, a traditional Chinese medical herb, is well known for its unique medical and edible value through the ages. Many types of compounds including saponins, flavonoids, alkaloids, lignins, polysaccharides, and lectins can be isolated from *P. sibiricum*. Saponins in *P. sibiricum*, especially the steroid saponins, have been proved to have various biological activities, such as anti-inflammatory, antimicrobial, hypoglycemic, and immunoregulatory activities. Previous study reported the separation of isonarthogenin 3-O-β-d-glucopyranosyl-(1 → 4)-β-d-galactopyranoside from the rhizomes of *P. sibiricum* (Wang et al., 2016). Further, four new steroidal saponins with anti-inflammatory activity were isolated from *P. sibiricum* (Tang et al., 2019).

Methyl protodioscin (MPD) is one of the high-content saponins in the rhizomes of *P. sibiricum*. Several studies investigated the protection exerted by MPD against intestinal inflammation and airway inflammation (Zhang et al., 2015; Hee et al., 2015). Ma et al. indicated that MPD can prevent cardiovascular diseases by improving the expression level of ABCA1, increasing the LDL synthesis and by inhibiting the expression level of sterol regulatory element-binding protein to lower LDL and TG levels (Ma et al., 2015). Anti-cancer effect of MPD

* Corresponding author. School of Food Science and Biological Engineering, Hefei University of Technology, Hefei, 230009, People's Republic of China.
E-mail addresses: yilong.ma@hfut.edu.cn (Y.-L. Ma), ying_shuo_zhang@163.com (Y.-S. Zhang), zffs2012@mail.ahnu.edu.cn (F. Zhang), 1217461863@qq.com (Y.-Y. Zhang), kumarikiran@hfut.edu.cn (K. Thakur), zhangjianguo@hfut.edu.cn (J.-G. Zhang), zjwei@hfut.edu.cn (Z.-J. Wei).
[1] Co-first author.

https://doi.org/10.1016/j.fct.2019.110655
Received 31 May 2019; Received in revised form 28 June 2019; Accepted 29 June 2019
Available online 02 July 2019

has also been proved by numerous reports (He et al., 2005; Chen et al., 2018; Bai et al., 2014). From the previous study, it was clear that the semi-inhibitory concentration of MPD against breast cancer cells MCF-7 was 10.5 μM (He et al., 2005). Chen et al. found that MPD reduced the expression level of c-Myc, a gene that causes infinite proliferation in pancreatic cancer cells MIA PaCa-2 and PANC-1, leading to a reduction of glycolysis, thereby inhibited the development of pancreatic cancer (Chen et al., 2018). Bai et al. demonstrated that the proapoptotic mechanism of MPD in A549 cells was exerted by decreasing mitochondrial membrane potential, promoting mitochondrial cytochrome *c* (Cyt *c*) release, activating Caspase-3, down-regulating Bcl-2, and up-regulating bax (Bai et al., 2014).

However, the anti-cancer effects of MPD are well known in different cancer cells lines except the cervical cancer cells. Therefore, we evaluated the anti-cancer activity of MPD for proliferation inhibition and apoptosis in cervical Hela cells.

2. Materials and methods

2.1. Chemicals

DMEM high glucose medium and penicillin/streptomycin were purchased from HyClone (Logan, UT, USA) and fetal bovine serum (FBS) was procured from CLARK Bioscience (Seabrook, MD, USA). Primary antibodies and secondary antibodies were ordered from Cell Signaling Technology (Danvers, MA, USA). The Caspase inhibitors (Z-IETD-FMK and Z-LEHD-FMK) were obtained from MedChem Express (NJ, USA).

2.2. Preparation of MPD

MPD was extracted from the roots of *P. sibiricum*. The sliced *P. sibiricum* was ground into powder and dried to constant weight at 50 °C. After extraction by 80% ethanol for three times, petroleum ether and water-saturated n-butyl alcohol were used successively for the removal of lipid and the isolation of saponins. The obtained extract was separated by silica gel column chromatography with the mobile phase of trichloromethane-methyl alcohol-n-butyl alcohol-water (10:5:1:4, v/v/v/v) (Ou-yang et al., 2018). Sephadex LH-20 column chromatography with ethanol as eluent solvent was used for the further purification (Wang et al., 2001). The purity of sample was analyzed by HPLC (Waters, Milford, MA, USA) using Hyper 0DS2 C18 column (4.6 × 250 mm) with the following parameters: column temperature of 25 °C, mobile phase of acetonitrile: water (25:75, v/v), flow rate of 1.0 mL/min, and injection volume of 20 μL. To determine the molecular weight of the compound, UPLC-TOF-MS/MS (Waters, Milford, MA, USA) with ESI source operated in the positive ion mode was adopted with a source temperature of 150 °C. The ionization voltage and capillary voltage were 4.5 kV and 3.2 kV, respectively. Furthermore, ^{13}C (151 MHz) and ^{1}H (600 MHz) nuclear magnetic resonance (NMR, Agilent, USA) with Pyridine-*d5* as a solvent were adopted for the in-depth exploration of molecular structure (Yang et al., 2016).

2.3. Cell culture conditions

The human cervical cancer cell lines (Hela) and HEK293 cell lines were procured from Shanghai wei atlas biological technology co., LTD (Shanghai, China) and incubated in DMEM high glucose medium, supplemented with 10% FBS and 1% penicillin/streptomycin at 37 °C under 5% CO_2 and 95% air (Zhang et al., 2017).

2.4. MTT assay

Exponentially growing Hela cells and HEK293 cells were collected and seeded in a 96-well plate with the concentration of 5 × 10^4 cells/mL and the volume of 100 μL per well. After 12 h of incubation, different concentrations of MPD (0, 5, 10, 15, 20, 25, 30, 35, and 40 μM) were added for 24 h treatment. In addition, 40 μM of 5-fluorouracil (5-Fu) were used as a positive control. Further, 20 μL of MTT regent (5 mg/mL) was supplemented into the medium and the cells were kept in 37 °C for 4 h. After incubation, the medium was substituted with 150 μL of DMSO to dissolve the formazan crystals prior to absorbance measurement at the wavelength of 570 nm (Wang et al., 2018).

Table 1
Primers for qPCR.

Gene	Primer	Sequence (5′-3′)
p53	Forward	AGCACTGTCCAACAACACCA
	Reverse	CTTCAGGTGGCTGGAGTGAG
p21	Forward	GCGGAACAAGGAGTCAGACA
	Reverse	GAACCAGGACACATGGGGAG
CyclinB1	Forward	CTGCTGGGTGTAGGTCCTTG
	Reverse	TGCCATGTTGATCTTCGCCT
CDK1	Forward	TTGAAACTGCTCGCACTTGG
	Reverse	TCCCGGCTTATTATTCCGCG
survivin	Forward	GGCCCAGTGTTTCTTCTGCT
	Reverse	ATGAGGGTGGAAAGCAACCC
Wee1	Forward	CTGAACAATGGGCCTCGTCT
	Reverse	ATCCTATGGCTCGGGAGTGT
Fas	Forward	GCAGGCCAAGTTGCTGAATC
	Reverse	CGTAAACCGCTTCCCTCACT
FADD	Forward	GGGAAGAAGACCTGTGTGCA
	Reverse	ATTCTCAGTGACTCCCGCAC
Caspase-3	Forward	TGGACTGTGGCATTGAGACA
	Reverse	CAGGTGCTGTGGAGTATGCA
Caspase-8	Forward	TATCCCGGATGGCTGACT
	Reverse	GACATCGCTCTCAGGCTC
Caspase-10	Forward	CAGGGGCAGGAAGAGAACAG
	Reverse	ACTAGGAAACGCTGCTCCAC
Bak	Forward	ACTCTACCCCTGCTCCCATT
	Reverse	CTTGGAGGCTTCTGACACGT
Bcl-xl	Forward	GCATTGTGGCCTTTTTCTCC
	Reverse	GCTGCTGCATTGTTCCCATA
puma	Forward	ATGCCTGCCTCACCTTCATC
	Reverse	TCAGCCAAAATCTCCCACCC
Cyt *c*	Forward	CCTCTGGGGCATTATCCATC
	Reverse	ATATTTGCACAGTGAAACATAGGA
Caspase-9	Forward	GCTCTTCCTTTGTTCATCTCC
	Reverse	CATCTGGCTCGGGGTTACTGC
β-actin	Forward	TGTGATGGTGGGAATGGGTCAG
	Reverse	TTTGATGTCACGCACGATTTCC

2.5. Cell cycle analysis

The effect of MPD treatment on Hela cells was determined by flow cytometry (FCM). The cells exposed to different concentrations (0, 6, 12, and 18 μM) of MPD for 24 h were assembled with a density of 1 × 10^6 cells/mL. After PBS washing, the cells were immobilized in 4 °C overnight using pre-cooling 70% ethanol. Then, the cells were re-suspended in cold propidium iodide (PI) solution for 30 min without exposure to light followed by flow cytometry (BD Accuri C6, USA) with the excitation wavelength of 488 nm.

2.6. Cell apoptotic analysis

Cell apoptotic analysis was conducted by using Annexin V-FITC/PI staining. The cells in the logarithmic growth phase were treated by different concentrations (0, 6, 12, and 18 μM) of MPD for 24 h and collected by trypsin without EDTA and washed with PBS primarily. Then after, the cells were suspended in 1 × Annexin V binding buffer with the concentration of 1 × 10^6 cells/mL prior to the staining of 5 μL of Annexin V-FITC at 2–8 °C in the dark. After staining for 15 min, 10 μL PI was added followed by 5 min incubation and treated cells were then detected by FCM.

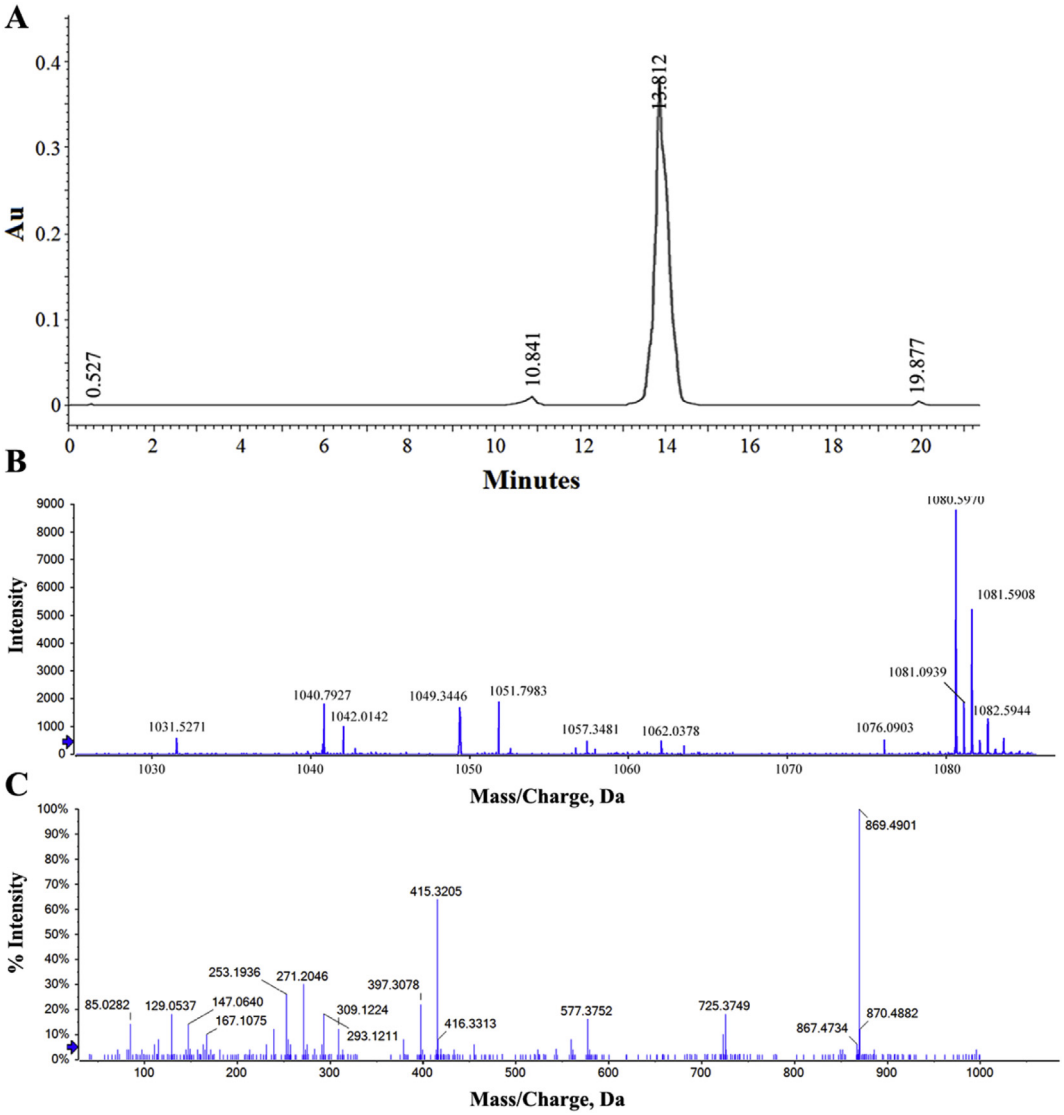

Fig. 1. Purity and molecular weight determination of the MPD. (A) HPLC chromatograms of MPD. (B) MS result of MPD. (C) MS/MS result of MPD.

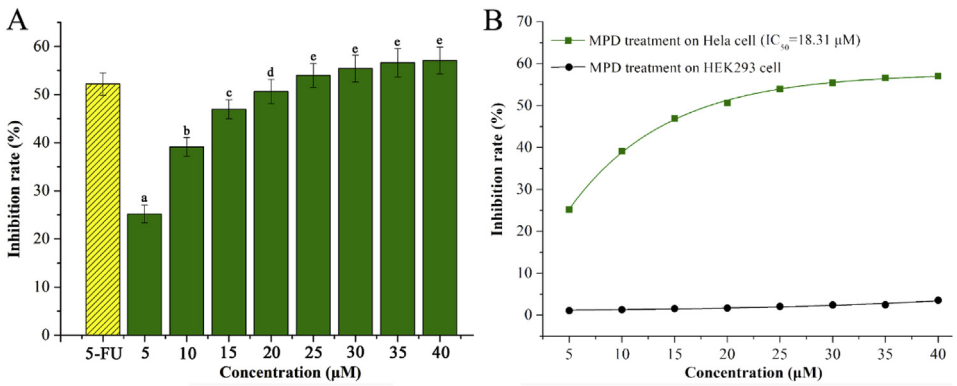

Fig. 2. The inhibitory effect of MPD on the proliferation of cells. (A) Inhibition of MPD and 5-Fu on the growth of HeLa cells (B) Fitted inhibition curve of HeLa and HEK293 cells treated with various concentrations of MPD. 5-fluorouracil (5-Fu) treatment (40 μM) was used as positive control. All cells were treated for 24 h. Data are presented as mean ± SD of three independent experiments. One-way ANOVA at $p < 0.05$ designated by superscript letters is used for statistical analysis.

2.7. Measurement of intracellular ROS accumulation

Series of MPD concentrations (0, 6, 12, and 18 μM) were prepared for the treatment of Hela cells in order to detect the reactive oxygen species (ROS) accumulation. The cells were treated for 24 h, collected with typsin and labeled using 10 μM fluorescence probe DCFH-DA (MedChem Express, NJ, USA) for 20 min at 37 °C. The accumulation of intracellular ROS was measured on the basis of the fluorescence intensity with FCM (Zhang et al., 2018b).

2.8. qPCR analysis

Hela cells were exposed to different concentrations of MPD (0, 6, 12, and 18 μM) for 24 h prior to collection and total RNA extraction.

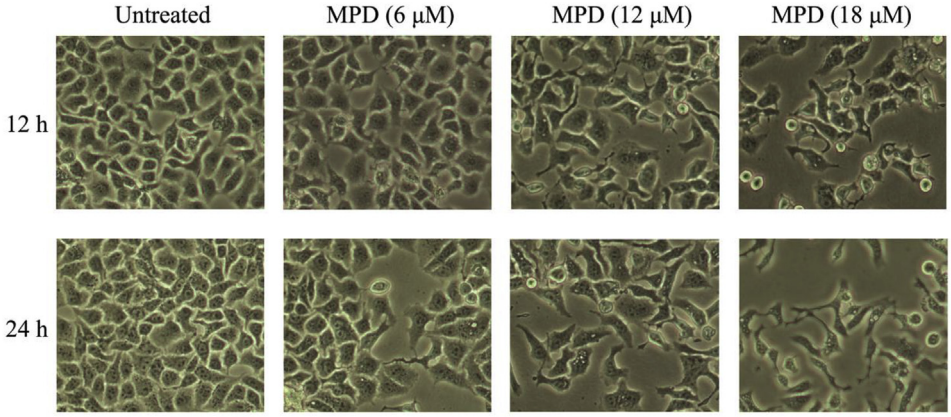

Fig. 3. Morphological changes in Hela cells treated with different concentrations of MPD (6, 12, and 18 μM) for 12 h or 24 h compared to untreated group. The images were observed by inverted optic microscope (original magnification × 200).

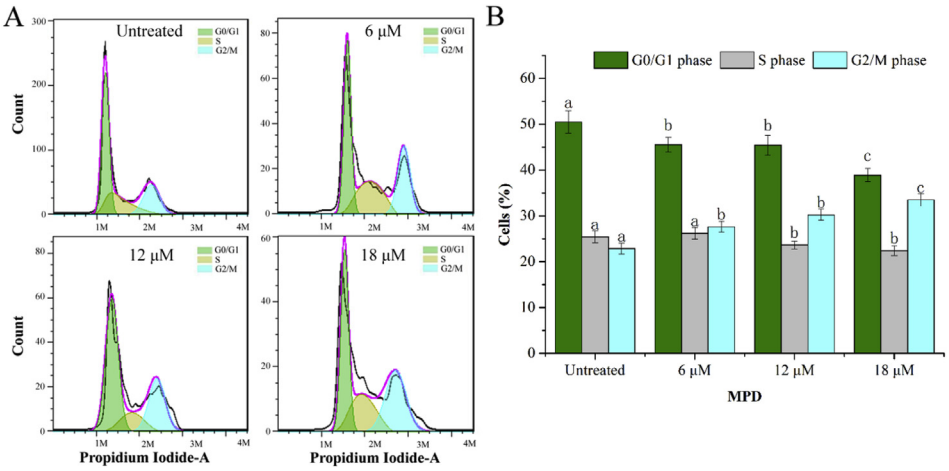

Fig. 4. MPD induced cell cycle arrest at G2/M phase in Hela cell lines. (A) Cell cycle distribution of Hela cells staining with PI was monitored by FCM after MPD-treatment. (B) The rate of cell cycle in different phases. One-way ANOVA at $p < 0.05$ designated by superscript a, b, c, d is used for statistical analysis.

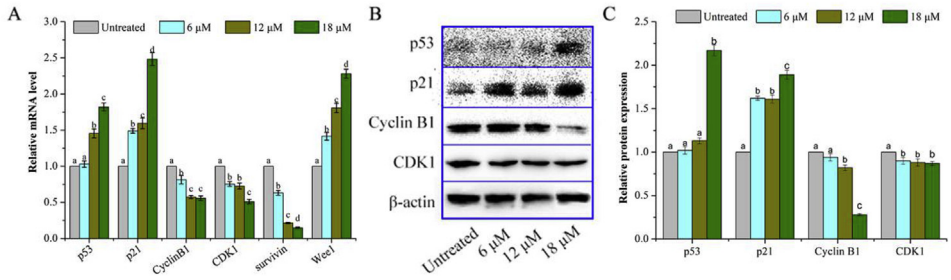

Fig. 5. The qPCR and Western blot analysis of the expression levels of cell cycle related genes and proteins with or without MPD treatment of Hela cells. (A) The effects of MPD on mRNA expression of cell cycle related genes in Hela cell investigated by qPCR. (B) The effects of MPD on cell cycle related proteins in Hela cell investigated by Western blot. (C) The expression levels of cell cycle related proteins. Data are presented as mean ± SD of three independent experiments. One-way ANOVA at $p < 0.05$ designated by superscript a, b, c, d is used for statistical analysis.

Reverse transcriptase kit (Takara, Japan) was used for the reverse transcription of total RNA to cDNA. The qPCR was performed by LightCycler 96 System (Roche, Basel, Switzerland). β-actin was used as reference gene. The nucleotide sequences of the related primers used in this study are listed in Table 1.

2.9. Western blot analysis

After 24 h treatment by MPD, Hela cells were collected and disrupted with RIPA lysis buffer (containing 1% PMSF protease inhibitors) to isolate proteins. Proteins associated with cell cycle and cell apoptosis were detected using primary antibodies specific for p53, p21, Cyclin B1, CDK1, Fas, Bak, Bcl-xl, Caspase-3, 8, 9 and β-actin. These operations were followed by incubation with HRP-tagged secondary antibodies at 37 °C for 1 h. ECL development was performed further to measure the relative expression levels of the proteins which were introduced previously (Zhang et al., 2017).

2.10. Statistical analysis

Data were expressed as mean ± SD (n ≥ 3) and analyzed using SPSS 20.0 software (SPSS, Inc., Chicago, IL, USA). Statistical significance among various treatments was assessed by using One-way analysis of variance (ANOVA) with significance level of $p < 0.05$.

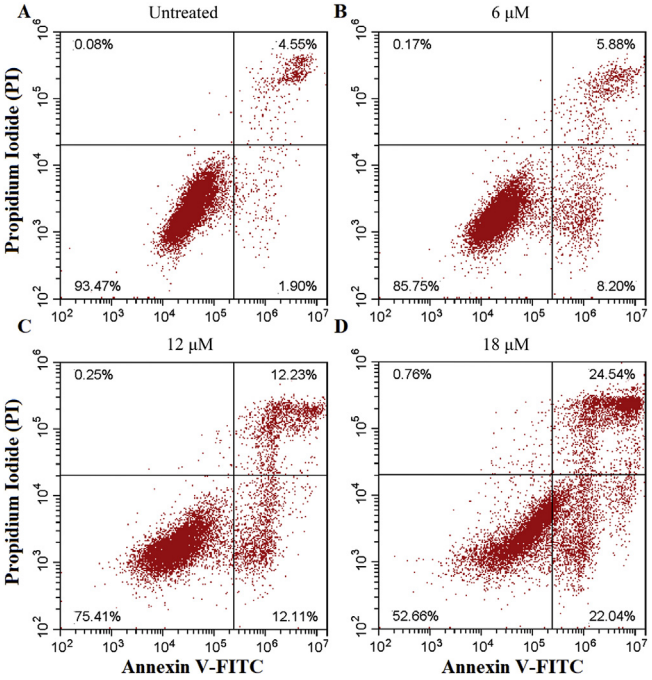

Fig. 6. Apoptosis induced by MPD in Hela cells was assessed by FCM analysis after staining with Annexin V-PI. (A, Untreated, B, 6 μM, C, 12 μM, D, 18 μM).

3. Results

3.1. MPD extraction from P. sibiricum

As shown in Fig. 1A, the obtained saponin was eluted with the retention time of 13.8 min and with the purity of 95.13% detected by HPLC analysis. According to the UPLC-TOF-MS/MS results, $[M + NH_4]^+$ peak at *m/z* 1081 illustrated that the molecular weight of the compound was 1063 Da (Fig. 1B and C). The structure of the product was identified using NMR (Supplementary Fig. 1). The multiple peak data of ^{13}C and ^{1}H were as follows: ^{13}C NMR (151 MHz, Pyridine-*d5*) δ: 148.46, 148.43, 148.27, 139.39, 134.26, 134.10, 133.93, 122.26, 122.10, 121.91, 120.38, 111.23, 103.57, 101.48, 100.61, 98.87, 79.88, 77.22, 77.10, 76.68, 76.53, 76.37, 75.51, 73.77, 72.71, 72.50, 71.41, 71.32, 71.13, 70.34, 68.99, 68.09, 62.75, 61.48, 59.87, 55.14, 48.89, 45.85, 39.36, 39.06, 37.56, 35.69, 32.80, 30.75, 30.22, 29.37, 26.75, 17.97, 17.22, 17.07, 15.72, 14.87, 14.83. ^{1}H NMR (600 MHz, Pyridine-*d5*) δ: 7.50 (s, 4H), 6.36 (s, 3H), 5.99 (d, *J* = 1.5 Hz, 6H), 5.58-5.55 (m, 4H), 5.45 (s, 1H), 5.18 (d, *J* = 1.5 Hz, 1H), 5.08 (s, 1H), 4.64 (d, *J* = 1.8 Hz, 1H), 4.10 (dd, *J* = 12.3, 4.8 Hz, 1H), 3.78-3.72 (m, 2H), 3.75-3.67 (m, 2H), 3.66-3.57 (m, 2H), 3.46 (dd, *J* = 3.4, 1.7 Hz, 1H), 3.41 (dd, *J* = 9.3, 3.4 Hz, 1H), 3.34 (ddd, *J* = 19.8, 10.5, 3.0 Hz, 2H), 3.27-3.08 (m, 5H), 3.02 (dp, *J* = 10.3, 7.1, 5.5 Hz, 5H), 2.87 (dd, *J* = 12.2, 3.5 Hz, 1H), 2.85-2.78 (m, 1H), 2.78-2.70 (m, 2H), 2.66 (ddt, *J* = 10.8, 7.6, 4.4 Hz, 1H), 2.45-2.35 (m, 2H), 2.05 (s, 2H), 1.62-1.56 (m, 1H), 1.50 (t, *J* = 12.3 Hz, 1H), 1.00 (tt, *J* = 10.0, 4.8 Hz, 1H), 0.89-0.72 (m, 3H), 0.74-0.64 (m, 2H), 0.54 (dd, *J* = 17.4, 7.6 Hz, 6H), 0.52-0.44 (m, 1H), 0.41 (d, *J* = 6.1 Hz, 3H), 0.25 (dddd, *J* = 58.4, 31.8, 11.7, 5.2 Hz, 2H), 0.21 (s, 3H), 0.12 (dd, *J* = 7.8, 3.9 Hz, 1H), −0.11–0.28 (m, 7H), −0.28–0.37 (m, 2H), −0.40 (s, 2H). After comparison, it was found that the chemical shift of the compound was consistent with the previous literature (Bah et al., 2004). Therefore, the compound isolated from *P. sibiricum* was identified as MPD.

3.2. Inhibitory effect of MPD on cell proliferation

The inhibitory effect of MPD on cell proliferation was detected using MTT assay. Treatment of MPD for 24 h could suppress the proliferation of Hela cells in a dose-dependent manner (Fig. 2A). 5-Fu, considered as a positive control, maintained the inhibition rate at 52.21%. According to the fitting curve, the IC_{50} of MPD on Hela cells was calculated as 18.31 μM (Fig. 2B). However, MPD almost displayed no inhibition to HEK293 cell line, with 4.59% inhibition rate at 40 μM after treatment for 24 h, which is dramatically lower than that in Hela cells (57.06%).

3.3. Effect of MPD on cell morphology

The morphology of Hela cells in the untreated group was polygonal and cells were closely arranged at different time points (Fig. 3). When treated with 6 μM of MPD, the morphology and number of cells did not change significantly after 12 h. However, when processing time extended to 24 h, the number of cells decreased and dead cells began to appear. Clearly, at the concentration of 12 μM, the cell morphology changed, the cytoplasm shrunk, and the number of dead cells increased. After treatment with 18 μM of MPD, majority of cells shrunk significantly, and some cells turned around simultaneously. A large number of cells were devitalized, presenting highly non-uniform shapes with multiple pseudopods extension. With the prolongation of treatment time, the drug was considered more effective.

3.4. Effect of MPD on cell cycle

In order to verify the anti-cancer activity, FCM was performed to detect the change of percentage in different phases of cell cycle caused by MPD treatment. As shown in Fig. 4, compared with the untreated group, the cells in G2/M phase increased significantly (27.60% for 6 μM MPD treatment, 30.20% for 12 μM, and 33.48% for 18 μM), accompanied by a concomitant decrease in G0/G1 phase, indicating that exposure to MPD for 24 h could result in cell cycle repression in G2/M phase.

Further examination was carried out to explore the molecular mechanism of MPD-induced cell cycle blocking in Hela cells. Fig. 5A revealed that different concentrations of MPD treatment could down regulate the mRNA levels of survivin, Cyclin B1, and CDK1, while it could increase the expression of p53, p21, and Wee1. Further, related proteins also showed a consistent trend (Fig. 5B and C), providing a strong basis for the effect of MPD on cell cycle.

3.5. Effect of MPD on cancer cell apoptosis

HeLa cells were exposed to different concentrations of MPD (0, 6, 12, and 18 μM) for 24 h, followed by staining with Annexin V-FITC and PI for FCM analysis. As shown in Fig. 6, the proportions of early apoptotic cells were 1.90%, 8.20%, 12.11%, and 22.04%, respectively. And the percentage of total apoptotic cells in treatment groups (4.08% for 6 μM, 24.34% for 12 μM and 46.58% for 18 μM) was apparently higher than that of untreated group. The results showed that MPD could induce apoptosis of Hela cells in a dose-dependent manner.

3.6. Effect of MPD on ROS generation

Fluorogenic probe DCFH-DA was used through FCM to analyze ROS generation in Hela cells. After treatment with different concentrations (0, 6, 12, and 18 μM) of MPD, the percentage of ROS positive cells increased from 1.15 ± 0.04% to 7.95 ± 0.17%, 32.20 ± 1.40% and 63.05 ± 2.24%, respectively, indicating that the apoptosis triggered by MPD may be related to the elevated levels of intracellular ROS (Fig. 7).

3.7. Effects of MPD on death receptor pathway

Death receptor-mediated extrinsic pathway is considered as a critical pathway for inducing cell apoptosis. Fig. 8 showed that MPD treatment affected the levels of mRNA and proteins associated with

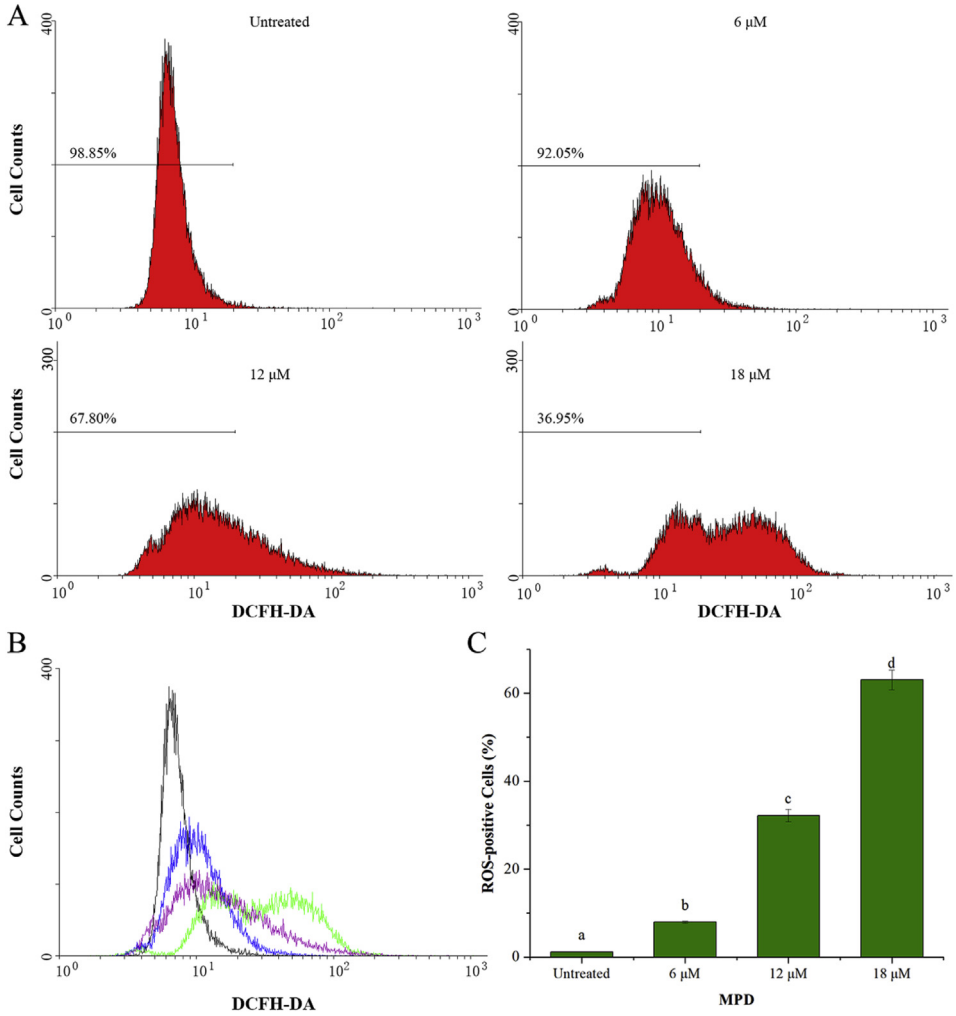

Fig. 7. MPD treatment caused ROS generation in Hela cells. (A) Cell distribution of untreated and MPD-treated Hela cells after DCFH-DA staining. (B) Trend diagram of ROS generation. (C) The percentage of ROS-positive cells for various concentrations of MPD treatment. Data are presented as mean ± SD of three independent experiments. One-way ANOVA at $p < 0.05$ designated by superscript a, b, c, d is used for statistical analysis.

death receptor pathway to a greater extent. The mRNA expression levels of death receptor pathway-related genes were generally increased. Similarly, the levels of Fas, Caspase-3, and Caspase-8 proteins were up-regulated with the increasing concentration of MPD.

Z-IETD-FMK is recognized as a Caspase-8 specific inhibitor (Huo et al., 2004). The adherent cells were firstly treated with Z-IETD-FMK and then exposed to 18 μM of MPD for 24 h. Compared to the MPD treated group, the expressions of Caspase-8 and Caspase-3 were decreased significantly in the inhibitor-processing group (Fig. 8D). These results verified that MPD-induced apoptosis in Hela cells was dependent upon Caspase-8 activation.

3.8. Effects of MPD on mitochondrial pathway

Another major pathway that induces apoptosis is mitochondrial pathway, also known as intrinsic pathway. In the present study, the expression of Bak, a pro-apoptotic member, was up-regulated significantly, while a downward trend was noticed for the expression level of anti-apoptotic Bcl-xl. As shown in Fig. 9, MPD could also increase the mRNA expression of puma gene and Cyt *c* gene. Besides, Caspase-9, considered as the key initiative caspase in mitochondrial pathway, was further activated when the concentration of MPD was higher than 12 μM.

To further investigate the effect of MPD on mitochondrial pathway, the pretreated cells using Caspase-9 specific inhibitor (Z-LEHD-FMK) were exposed to 18 μM MPD for 24 h (Cao et al., 2010). The expression levels of Caspase-9 and Caspase-3 were lowered than that of MPD-treated group, even less than untreated group as shown in Fig. 9, indicating that MPD induced apoptosis in Hela cells was closely linked to mitochondrial pathway.

After analyzing our data based on different parameters, a probable molecular mechanism for the anti-cancer activities of MPD on cell cycle and apoptosis in Hela cells is presented in Fig. 10.

4. Discussion

The steroidal saponins in *P. sibiricum* are usually extracted using ethanol and n-butanol and isolated by multi-stage column chromatography (Wang et al., 2016; Zhang et al., 2018a). For the further study of the structure of purified saponins, various methods such as HPLC, UPLC-TOF-MS/MS and NMR are often used (Tang et al., 2019; Xu et al., 2009). Herein, we prepared and identified the MDP from *P. sibiricum* through aforementioned method.

It is suggested that the morphological alterations in cancer cells treated with anticancer drugs would help in evaluating their efficacy (Zhou et al., 2008). In our investigation, cytoplasm shrinks and cellular destruction occurred when the cells were exposed to MPD. Wang et al. observed that MPD treatment on HepG2 cells can lead to cytoplasm shrinkage, nuclear condensation, and cellular structure fragmentation (Wang et al., 2006), which were much similar to our observations.

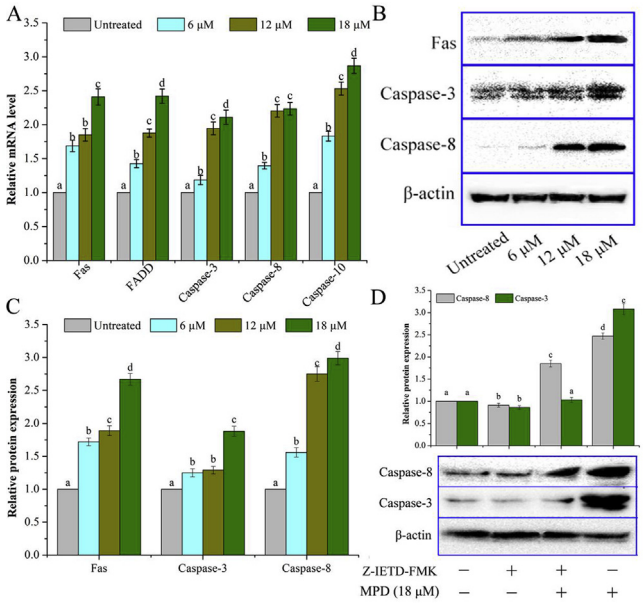

Fig. 8. The expression levels of death receptor pathway related genes and proteins in MPD (0, 6, 12 μM and 18 μM) treated Hela cells. (A)The mRNA expression levels of death receptor pathway related genes in MPD treated Hela cells. (B) The effects of MPD on death receptor pathway related proteins in Hela cells. (C) The expression levels of death receptor pathway related proteins in Hela cells. (D) The effects of MPD on apoptosis in Hela cells treated with or without Caspase-8 inhibitor. Data are presented as mean ± SD of three independent experiments. One-way ANOVA at $p < 0.05$ designated by superscript a, b, c, d is used for statistical analysis.

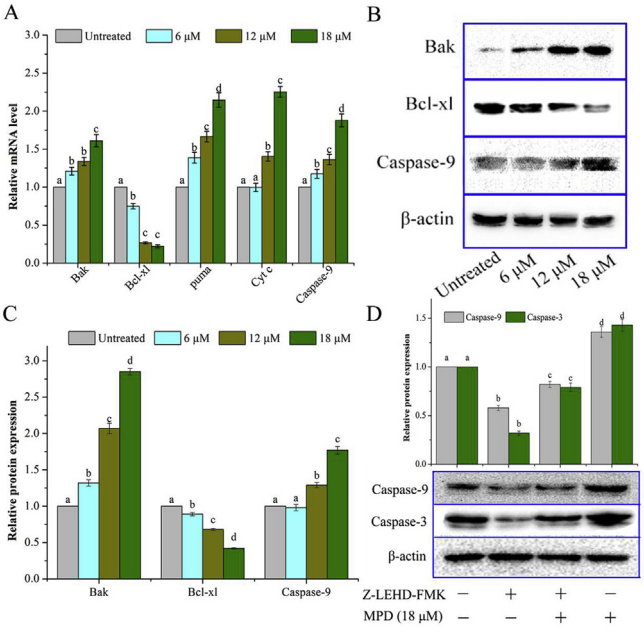

Fig. 9. The expression levels of mitochondrial pathway related genes and proteins in Hela cells treated with increasing concentrations of MPD (6, 12 and 18 μM). (A) The mRNA expression levels of mitochondrial pathway related genes in Hela cells. (B) The effects of MPD on mitochondrial pathway related proteins in Hela cells. (C) The expression levels of mitochondrial pathway related proteins. (D) The effects of MPD on apoptosis in Hela cells treated with or without Caspase-9 inhibitor. Data are presented as mean ± SD of three independent experiments. One-way ANOVA at $p < 0.05$ designated by superscript a, b, c, d is used for statistical analysis.

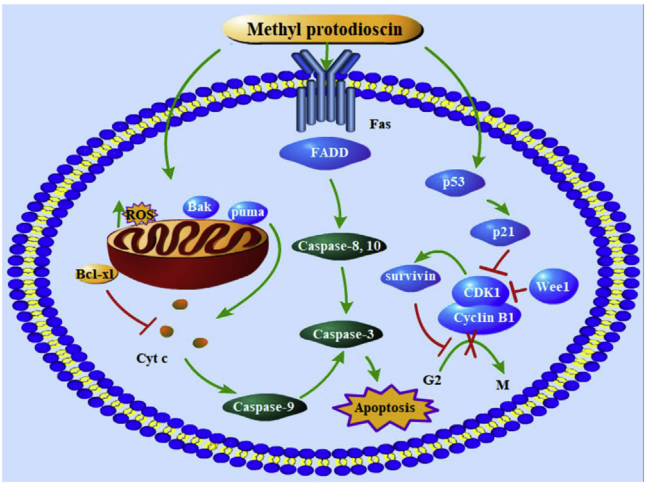

Fig. 10. Probable molecular mechanism for the anti-cancer activities of MPD on cell cycle and apoptosis in Hela cells.

The alteration of cell cycle progression may lead to cytokinesis failure and the consequent cell death (Wang et al., 2010). Anticancer drugs usually exert their effects by obstructing the cell division cycle through interaction with cell cycle-associated targets (Altinok et al., 2007). MPD treatment could increase the percentage of cells in G2/M phase from 22.34% to 33.48% according to our measurement, exerting cell cycle arrest effect on Hela cells. It can bind directly to Bcl-xl in the Bcl-2 family to inhibit the activity of anti-apoptotic protein and regulated apoptotic pathway (Lee et al., 2008; El-Garawani et al., 2019). The p21 gene is a vital member in the family of CDK inhibitors. It can adjust the relationship between cell cycle, DNA replication, and repair by repressing the activity of CDK complexes, which is closely related to tumor suppression and cell cycle control processes (Karimian et al., 2016). External stimuli regulate cell cycle via a p53-dependent pathway, in which p53 activates its downstream factor, p21, and the combination of p21 and CDK1-Cyclin B1 complex prevents CDK activation, leading to cell cycle arrest (Wang et al., 2019). In addition, some other regulatory factors, such as survivin and Wee1, are implicated in the coordination of cell cycle (Li et al., 2015). Survivin, considered as a CDK1 target, is almost undetectable in most differentiated normal cells, while abnormally elevated in most cancers (Goga et al., 2007). As a centromere-associated carrier protein, survivin plays a role in regulating cell division. The destruction of survivin in cells prolongs the middle stage of mitosis, induces polyploid production, and blocks the cell cycle at G2/M phase (Fukuda et al., 2004). Whereas, Wee1 is a nuclear tyrosine kinase that negatively regulates the activity of CDK1 and prevents mitosis from entering DNA synthesis (Yang et al., 2004). Previously, studies have shown that MPD can repress cell cycle in G2/M phase (Bai et al., 2014; Liu et al., 2005). Wang et al. (2006) proved that MPD-induced cell cycle repression was closely related to the decrease of Cyclin B1. Hsieh et al. (2017) proved that MPD increased the cell population of G2/M phase in SAS and SCC9 cells through the decrease of CDK1, Cyclin B1, and the increase of p21. Moreover, Similarly, Tseng et al. (2017) investigated the blocking effect of MPD on G2/M phase of human osteosarcoma cells. In the present study, MPD treatment decreased the expression of Cyclin B1 and CDK1, and on the contrary, the expression levels of p53 and p21 were significantly increased. These phenomena demonstrated that MPD could induce cell cycle arrest in G2/M phase.

Apoptosis has become the focus of investigation on innovative anticancer compounds. Hence, detection of apoptotic cells was accomplished for determining the anticancer effect of MPD. After exposure to MPD for 24 h, the rate of apoptotic cells elevated from 4.08% to 46.58%. To further confirm the mechanism of apoptosis induced by MPD, intracellular ROS levels were detected, and a significant increase

of ROS levels were found after 24 h of MPD-treatment. ROS are a class of greatly reactive ions and molecules involved in the regulation of various biological processes (Zhang et al., 2018c). They are usually present in the form of hydrogen peroxide, superoxide anion, and hydroxyl radicals in cells. ROS is associated with various metabolism disorders like cancer, diabetes, and cardiovascular diseases (Pi et al., 2015; Galadari et al., 2017). The accumulation of large amounts of ROS in the cells initiates the suppression of mitochondrial membrane potential, activates varies of pathways, like death receptor pathway and mitochondrial pathway, and drives the process of cell apoptosis ultimately.

MPD up-regulated the expression level of Fas, Caspase-3, and Caspase-8. Fas is firstly activated by its ligand and then lead to the binding of Fas-associated death domain (FADD). Once bound, the death domain can activate Caspase-8 and Caspase-10, and then in turn triggers the Caspase-3, which successively induces the programmed cell death (Yang et al., 2015).

Mitochondrial pathway is primarily controlled by the Bcl-2 family which contains anti-apoptotic, pro-apoptotic, and BH3-only members (Siddiqui et al., 2015). The remarkable changes in Bak and Bcl-xl, together with the increase of puma (BH3-only member), accelerated the release of Cyt *c* from mitochondria, which activated the initiator Caspase-9. Subsequently, Caspase-9 stimulated its downstream performer (Caspase-3), and then triggered the cell apoptosis. Chen et al. demonstrated the analogous proapoptotic mechanism of MPD in pancreatic cancer cells. It is reported that MPD down-regulated Bcl-2, up-regulated Bax, and led to apoptosis of MIA PaCa-2 and PANC-1 cells eventually (Chen et al., 2018).

5. Conclusions

Taken together, our study investigated the anticancer effect of MPD, a steroid saponin separated from *P. sibiricum*. The results showed that MPD treatment resulted in suppressed growth of cancer cells, altered the cell morphology, and blocked the cell cycle at G2/M phase and ultimately triggered the cell apoptosis. The main mechanisms of MPD-induced apoptosis were confirmed as the accumulation of intracellular ROS, the activation of death receptor pathway, and the promotion of mitochondrial pathway. Therefore, MPD possess the potential to be applied as natural anti-cancerous drug in therapeutic strategies.

Conflicts of interest

There is none to declare.

Acknowledgments

This work was supported by the National Natural Science Foundation of China (31850410476), the Major Projects of Science and Technology in Anhui Province (18030701144, 1804b06020347, 18030701142, 18030701158, 17030701028), and Fundamental Research Funds for the Central Universities (JZ2019HGTB0061).

Appendix A. Supplementary data

Supplementary data to this article can be found online at https://doi.org/10.1016/j.fct.2019.110655.

Transparency document

Transparency document related to this article can be found online at https://doi.org/10.1016/j.fct.2019.110655

References

Altinok, A., Levi, F., Goldbeter, A., 2007. A cell cycle automaton model for probing circadian patterns of anticancer drug delivery. Adv. Drug Deliv. Rev. 59, 1036–1053.
Bah, M., Gutierrez, D.M., Escobedo, C., Mendoza, S., Rojas, J.I., Rojas, A., 2004. Methylprotodioscin from the Mexican medical plant *Solanum rostratum* (Solanaceae). Biochem. Syst. Ecol. 32, 197–202.
Bai, Y., Qu, X.Y., Yin, J.Q., Wu, L.C., Jiang, H., Long, H.W., Jia, Q., 2014. Methyl protodioscin induces G2/M cell cycle arrest and apoptosis in A549 human lung cancer cells. Phcog. Mag. 10, 318–324.
Cao, W., Li, X.Q., Wang, X., Fan, H.T., Zhang, X.N., Hou, Y., Liu, S.B., Mei, Q.B., 2010. A novel polysaccharide, isolated from *Angelica sinensis* (Oliv.) Diels induces the apoptosis of cervical cancer HeLa cells through an intrinsic apoptotic pathway. Phytomedicine 17, 598–605.
Chen, L.Y., Cheng, C.S., Gao, H.F., Zhan, L., Wang, F.J., Qu, C., Li, Y., Wang, P., Chen, H., Meng, Z.Q., Liu, L.M., Chen, H.F., Chen, Z., 2018. Natural compound methyl protodioscin suppresses proliferation and inhibits glycolysis in pancreatic cancer. Evid-Based Compl. Alt. 2018, 7343090.
Daniyal, M., Akhtar, N., Ahmad, S., Fatima, U., Akram, M., Asif, H.M., 2015. Update knowledge on cervical cancer incidence and prevalence in Asia. Asian Pac. J. Cancer P. 16, 3617–3620.
El-Garawani, I.M., Elkhateeb, W.A., Zaghlol, G.M., Almeer, R.S., Ahmed, E.F., Rateb, M.E., Moneim, A.E.A., 2019. *Candelariella vitellina* extract triggers in vitro and in vivo cell death through induction of apoptosis: a novel anticancer agent. Food Chem. Toxicol. 127, 110–119.
Fukuda, S., Mantel, C.R., Pelus, L.M., 2004. Survivin regulates hematopoietic progenitor cell proliferation through p21WAF1/Cip1-dependent and -independent pathways. Blood 103, 120–127.
Galadari, S., Rahman, A., Pallichankandy, S., Thayyullathil, F., 2017. Reactive oxygen species and cancer paradox: to promote or to suppress? Free Radic. Biol. Med. 104, 144–164.
Goga, A., Yang, D., Tward, A.D., Morgan, D.O., Bishop, J.M., 2007. Inhibition of CDK1 as a potential therapy for tumors over-expressing. MYC. Nat. Med. 13, 820–827.
He, X.J., Wang, X.L., Liu, B., Su, L.N., Wang, G.H., Qu, G.X., Yao, Z.H., Liu, R.H., Yao, X.S., 2005. Microbial transformation of methyl protodioscin by *Cunninghamella elegans*. J. Mol. Catal. B Enzym. 35, 33–40.
Hee, L.J., Jai, L.H., Woo, L.C., Son, K.H., Son, J.K., Lee, S.K., Kim, H.K., 2015. Methyl Protodioscin from the roots of *Asparagus cochinchinensis* attenuates airway inflammation by inhibiting cytokine production. Evid-Based Compl. Alt. 2015, 640846.
Hsieh, M.J., Lin, C.W., Chen, M.K., Chien, S.Y., Lo, Y.S., Chuang, Y.C., Hsi, Y.T., Lin, C.C., Chen, J.C., Yang, S.F., 2017. Inhibition of cathepsin S confers sensitivity to methyl protodioscin in oral cancer cells via activation of p38 MAPK/JNK signaling pathways. Sci. Rep. 7, 45039.
Huo, R., Zhou, Q.L., Wang, B.X., Tashiro, S.I., Onodera, S., Ikejima, T., 2004. Diosgenin induces apoptosis in HeLa cells via activation of caspase pathway. Acta Petrol. Sin. 25, 1077–1082.
Karimian, A., Ahmadi, Y., Yousefi, B., 2016. Multiple functions of p21 in cell cycle, apoptosis and transcriptional regulation after DNA damage. DNA Repair 42, 63–71.
Kiraz, Y., Adan, A., Yandim, M.K., Baran, Y., 2016. Major apoptotic mechanisms and genes involved in apoptosis. Tumor Biol. 37, 8471–8486.
Lee, T.L., Yeh, J., Friedman, J., Yan, B., Yang, X.P., Yeh, N.T., Van, W.C., Chen, Z., 2008. A signal network involving coactivated NF-kappa B and STAT3 and altered p53 modulates BAX/BCL-XL expression and promotes cell survival of head and neck squamous cell carcinomas. Int. J. Cancer 122, 1987–1998.
Li, Y.H., Liu, D., Zhou, Y.L., Li, Y.J., Xie, J., Lee, R.J., Cai, Y., Teng, L.S., 2015. Silencing of survivin expression leads to reduced proliferation and cell cycle arrest in cancer cells. J. Cancer 6, 1187–1194.
Lin, C.C., Chuang, Y.J., Yu, C.C., Yang, J.S., Lu, C.C., Chiang, J.H., Lin, J.P., Tang, N.Y., Huang, A.C., Chung, J.G., 2012. Apigenin induces apoptosis through mitochondrial dysfunction in U-2 OS human osteosarcoma cells and inhibits osteosarcoma xenograft tumor growth in vivo. J. Agric. Food Chem. 60, 11395–11402.
Liu, M.J., Yue, P.Y.K., Wang, Z., Wong, R.N.S., 2005. Methyl protodioscin induces G2/M arrest and apoptosis in K562 cells with the hyperpolarization of mitochondria. Cancer Lett. 224, 229–241.
Ma, W.L., Ding, H., Gong, X.H., Liu, Z., Lin, Y.L., Zhang, Z.Z., Lin, G.R., 2015. Methyl protodioscin increases ABCA1 expression and cholesterol efflux while inhibiting gene expressions for synthesis of cholesterol and triglycerides by suppressing SREBP transcription and microRNA 33a/b levels. Atherosclerosis 239, 566–570.
Ou-yang, S.H., Jiang, T., Zhu, L., Yi, T., 2018. Dioscorea nipponica Makino: a systematic review on its ethnobotany, phytochemical and pharmacological profiles. Chem. Cent. J. 12, 57.
Pi, J., Cai, H.H., Jin, H., Yang, F., Jiang, J.H., Wu, A.G., Zhu, H.Y., Liu, J.X., Su, X.H., Yang, P.H., 2015. Qualitative and quantitative analysis of ROS mediated oridonin-Induced oesophageal cancer KYSE-150 cell apoptosis by atomic force microscopy. PLoS One 10, e0140935.
Siddiqui, W.A., Ahad, A., Ahsan, H., 2015. The mystery of BCL2 family: Bcl-2 proteins and apoptosis: an update. Arch. Toxicol. 89, 289–317.
Tang, C., Yu, Y.M., Qi, Q.L., Wu, X.D., Wang, J., Tang, S.A., 2019. Steroidal saponins from the rhizome of *Polygonatum sibiricum*. J. Asian Nat. Prod. Res. 21, 197–206.
Tseng, S.C., Shen, T.S., Wu, C.C., Chang, I.L., Chen, H.Y., Hsieh, C.P., Cheng, C.H., Chen, C.L., 2017. Methyl protodioscin induces apoptosis in human osteosarcoma cells by caspase-dependent and MAPK signaling pathways. J. Agric. Food Chem. 65, 2670–2676.
Tsikouras, P., Zervoudis, S., Manav, B., Tomara, E., Iatrakis, G., Romanidis, C., Bothou, A., Galazios, G., 2016. Cervical cancer: screening, diagnosis and staging. J. Buon. 21, 320–325.
Wang, G., Chen, H.F., Huang, M.H., Wang, N.L., Zhang, J.C., Zhang, Y., Bai, G.R., Fong, W.F., Yang, M.S., Yao, X.S., 2006. Methyl protodioscin induces G2/M cell cycle arrest and apoptosis in HepG2 liver cancer cells. Cancer Lett. 241, 102–109.

Wang, H.C., Yang, J.H., Hsieh, S.C., Sheen, L.Y., 2010. Allyl sulfides inhibit cell growth of skin cancer cells through induction of DNA damage mediated G2/M arrest and apoptosis. J. Agric. Food Chem. 58, 7096–7103.

Wang, J., Lu, C.S., Liu, D.Y., Xu, Y.T., Zhu, Y., Wu, H.H., 2016. Constituents from *Polygonatum sibiricum* and their inhibitions on the formation of advanced glycosylation end products. J. Asian Nat. Prod. Res. 18, 697–704.

Wang, J., Liao, A.M., Thakur, K., Zhang, J.G., Huang, J.H., Wei, Z.J., 2019. Licochalcone B extracted from *Glycyrrhiza uralensis* Fisch induces apoptotic effects in human hepatoma cell HepG2. J. Agric. Food Chem. 67, 3341–3353.

Wang, J., Zhang, Y.S., Thakur, K., Hussaina, S.S., Zhang, J.G., Xiao, G.R., Wei, Z.J., 2018. Licochalcone A from licorice root, an inhibitor of human hepatoma cell growth via induction of cell apoptosis and cell cycle arrest. Food Chem. Toxicol. 120, 407–417.

Wang, Z., Zhou, J.B., Ju, Y., Zhang, H.J., Liu, M.J., Li, X., 2001. Effects of two saponins extracted from the *Polygonatum Zanlanscianense* Pamp on the human leukemia (HL-60) cells. Biol. Pharm. Bull. 24, 159–162.

Xu, D.P., Hu, C.Y., Zhang, Y., 2009. Two new steroidal saponins from the rhizome of *Polygonatum sibiricum*. J. Asian Nat. Prod. Res. 11, 1–6.

Yang, B.Y., Zhang, J., Liu, Y., Kuang, H.X., 2016. Steroidal saponins from the rhizomes of *Anemarrhena asphodeloides*. Molecules 21, 1075.

Yang, L., MacLellan, W.R., Han, Z.G., Weiss, J.N., Qu, Z.L., 2004. Multisite phosphorylation and network dynamics of cyclin-dependent kinase signaling in the eukaryotic cell cycle. Biophys. J. 86, 3432–3443.

Yang, T., Shi, R., Chang, L., Tang, K., Chen, K., Yu, G., Tian, Y., Guo, Y., He, W., Song, X., Xu, H., Ye, Z., 2015. Huachansu suppresses human bladder cancer cell growth through the Fas/Fasl and TNF-alpha/TNFR1 pathway in vitro and in vivo. J. Exp. Clin. Canc. Res. 34, 21–30.

Zhang, F., Zhang, J.G., Qu, J., Zhang, Q., Prasad, C., Wei, Z.J., 2017. Assessment of anticancerous potential of 6-gingerol (Tongling White Ginger) and its synergy with drugs on human cervical adenocarcinoma cells. Food Chem. Toxicol. 109, 910–922.

Zhang, H.Y., Hu, W.C., Ma, G.X., Zhu, N.L., Sun, X.B., Wu, H.F., Xu, X.D., 2018a. A new steroidal saponin from *Polygonatum sibiricum*. J. Asian Nat. Prod. Res. 20, 586–592.

Zhang, Q., Zhang, F., Thakur, K., Wang, J., Wang, H., Hu, F., Zhang, J.G., Wei, Z.J., 2018b. Molecular mechanism of anti-cancerous potential of Morin extracted from mulberry in Hela cells. Food Chem. Toxicol. 112, 466–475.

Zhang, R.L., Gilbert, S., Yao, X.S., Vallance, J., Steinbrecher, K., Moriggl, R., Zhang, D.S., Eluri, M., Chen, H.F., Cao, H.Q., Shroyer, N., Denson, L., Han, X.N., 2015. Natural compound methyl protodioscin protects against intestinal inflammation through modulation of intestinal immune responses. Pharmacol. Res. Perspect. 3, 118.

Zhang, Y.S., Ma, Y.L., Thakur, K., Hussain, S.S., Wang, J., Zhang, Q., Zhang, J.G., Wei, Z.J., 2018c. Molecular mechanism and inhibitory targets of dioscin in HepG2 cells. Food Chem. Toxicol. 120, 143–154.

Zhou, D.X., Jiang, X.D., Xu, R.X., Cai, Y.Q., Hu, J.L., Xu, G., Zou, Y.X., Zeng, Y.Z., 2008. Assessing the cytoskeletal system and its elements in C6 glioma cells and astrocytes by atomic force microscopy. Cell. Mol. Neurobiol. 28, 895–905.